Surface dielectric response of a semimetal: Electron-energy-loss spectroscopy of graphite

James F. Annett, R. E. Palmer, and R. F. Willis
Cavendish Laboratory, Madingley Road, Cambridge CB3 0HE, United Kingdom
(Received 17 July 1987)

The surface-dielectric-response function is important in describing a wide range of many-body properties of surfaces. Previous calculations of this quantity have assumed a free-electron metal surface, treated in a jellium approximation. Here we present calculations of the dielectric-response function of a graphite surface. These calculations show that the dielectric behavior of the graphite surface is quite different from that of simple metals. Using the calculated surface dielectric function we obtain theoretical electron-energy-loss spectra of graphite in the 0–1.4 eV range, which compare well with the experimental data. The spectra have a number of unusual features that are shown to be consequences of the semimetallic band structure and the kinematics of the dipole-scattering theory.

A number of important many-body phenomena in surface science involve a long-ranged interaction between a surface and an external probe, which might be an electron, an ion, a neutral atom, or another surface. Such interactions can always be formulated in terms of a dielectric function, $g(\mathbf{q}_\parallel,\omega)$, which characterizes the linear response of the surface to external fields.[1,2] For example, using a self-energy formalism one can express the image potential of an ion,[3] or the van der Waals potential of an atom, near a surface as an integral over $\mathbf{q}_\parallel$ and ω where the integrand contains the imaginary part of the surface dielectric function $\mathrm{Im}[g(\mathbf{q}_\parallel,\omega)]$.[4,5] Similarly, in electron-energy-loss spectroscopy (EELS), the probability that an electron reflected from the surface loses an energy $\hbar\omega$ and parallel momentum $\hbar\mathbf{q}_\parallel$ is proportional to the same dielectric function $\mathrm{Im}[g(\mathbf{q}_\parallel,\omega)]$.[1,2,6–8] The calculation of the surface dielectric function $\mathrm{Im}[g(\mathbf{q}_\parallel,\omega)]$ is thus an important task in theoretical surface physics [note that it is sufficient to calculate the imaginary part of $g(\mathbf{q}_\parallel,\omega)$, since the real part can then be found from a Kramers-Kronig relation]. To date, calculations of this quantity have assumed a free-electron metal substrate, treated in the jellium approximation. In this paper we shall calculate the surface dielectric function $\mathrm{Im}[g(\mathbf{q}_\parallel,\omega)]$ for a semimetal, graphite, where the details of the band structure near the Fermi level give rise to a dielectric response which is very different from a free-electron metal.

The motivation for this work is provided by the very unusual electron-energy-loss spectra that have been observed recently on a graphite surface.[9,10] As described in Ref. 9 the spectra show a broad background of electron-hole pair excitation losses extending continuously from 0 to beyond 1.4 eV. One unusual feature of this background is its specular intensity; it is 2 orders of magnitude stronger than the corresponding spectrum for a typical metallic substrate. This high intensity is particularly surprising given the low density of states for graphite near the Fermi energy. The nonspecular spectra also show anomalous dispersing loss structures which are not associated with any single energy loss channel. We have shown previously[9] that both the specular high intensity and the unusual features of the nonspecular spectra can be explained in terms of the semimetallic band structure of graphite near the Fermi level and the kinematics of the long-ranged dipole scattering theory. In Ref. 9 we summarized calculations of the EELS intensities carried out using a theoretical surface dielectric function derived for graphite, which gave a good overall agreement with the experimental results. The purpose of this paper is to present these calculations in more detail, especially the method of obtaining the surface dielectric function for graphite since previous calculations have only applied to metallic substrates. This calculation also explicitly demonstrates the relationship between the surface dielectric response of graphite and the semimetallic electronic structure.

The graphite surface is intrinsically interesting since it shows a number of peculiar properties. Among these anomalous features are the very large surface corrugations of several angstroms observed in the scanning tunneling microscope (STM),[11] and the strong asymmetry of the STM image which shows only one of the two surface atoms in each unit cell.[12] The unusual EELS spectrum is another example of a surface property of graphite where the semimetallic band structure leads to behavior which is quite different from either a metal or a semiconductor.

THE SURFACE-DIELECTRIC-RESPONSE FUNCTION

In this section we shall first review the definition of the surface dielectric function, and then outline the basic approximations that can be used to calculate it. In the following section we show how the surface dielectric function can be calculated for a material such as graphite with a nonmetallic band structure. Finally, we discuss some implications of this calculation and comparison with experimental data, especially for the EELS spectrum. In the Appendix we describe how the relationship between the EELS intensities and the imaginary

part of the surface dielectric function arises as a consequence of long-range dipole scattering.

The surface dielectric function $g(\mathbf{q}_\parallel,\omega)$ can be defined in the following way.[1] Assuming the solid occupies the half space $z<0$, then any external charges in $z>0$ will give rise to a field $\phi_{\rm ext}$ which can be Fourier decomposed into fields of the form

$$\phi_{\rm ext}(\mathbf{r},t)\equiv A(\mathbf{q}_\parallel,\omega)\exp(i\mathbf{q}_\parallel\cdot\mathbf{r}_\parallel+q_\parallel z-i\omega t) \tag{1a}$$

in the region $z\le 0$, where $\mathbf{q}_\parallel$ is a two-dimensional wave vector in the plane parallel to the surface, $\mathbf{r}=(\mathbf{r}_\parallel,z)$, and $q_\parallel=|\mathbf{q}_\parallel|$. The exponential z dependence is required in order to satisfy the relation $\nabla^2\phi_{\rm ext}=0$ in $z\le 0$. Since all the induced charges will lie in the half space $z<0$ the induced field must be of the form

$$\phi_{\rm ind}(\mathbf{r},t)=-g(\mathbf{q}_\parallel,\omega)A(\mathbf{q}_\parallel,\omega)\exp(i\mathbf{q}_\parallel\cdot\mathbf{r}_\parallel-q_\parallel z-i\omega t) \tag{1b}$$

in the region $z>0$, again to satisfy $\nabla^2\phi_{\rm ind}=0$ in $z>0$. We are neglecting local fields effects here (i.e., induced fields varying like $\exp[i(\mathbf{q}_\parallel+\mathbf{G}_\parallel)\cdot\mathbf{r}_\parallel]$ with $\mathbf{r}_\parallel$, where $\mathbf{G}_\parallel$ is a two-dimensional reciprocal lattice vector of the surface). The local fields will be unimportant if we are only interested in the response in the small $\mathbf{q}_\parallel$ region. These relations, Eq. (1), define the surface-dielectric-response function $g(\mathbf{q}_\parallel,\omega)$. The surface dielectric function thus completely characterizes the fields induced outside the surface by polarization caused by external charges. As a simple example, which will also be of use below, note that in the $q_\parallel\to 0$ limit we can treat the solid as a classical dielectric terminated at $z=0$. Solving the classical electrostatics problem of an ideal dielectric with a surface at $z=0$ gives

$$g(0,\omega)=\frac{\epsilon(\omega)-1}{\epsilon(\omega)+1}\ , \tag{2}$$

where $\epsilon(\omega)$ is the bulk dielectric constant. It is also possible to solve the classical problem for an anisotropic dielectric such as graphite; in this case, Eq. (2) still holds but with $\epsilon(\omega)=\sqrt{(\epsilon_1\epsilon_3)}$, where $\epsilon_1(\omega)$ and $\epsilon_3(\omega)$ are the dielectric functions for fields polarized, respectively, perpendicular to or parallel to the graphite c axis (assumed normal to the surface).

In standard linear response theory the induced charges, and hence the induced fields, can be related to the density response function $\chi(\mathbf{r},\mathbf{r}',\omega)$ of the solid. $\chi(\mathbf{r},\mathbf{r}',\omega)$ is defined so that the induced charge is given by $\rho_{\rm ind}=\chi\cdot\phi_{\rm ext}$, where, for brevity, we adopt a notation used in Ref. 13 in which functions such as $\phi_{\rm ext}(\mathbf{r}')$ are treated as Hilbert space vectors and $\chi(\mathbf{r},\mathbf{r}',\omega)$ becomes a matrix χ; the vector dot product then corresponds to integration over $\mathbf{r}$. Thus in this notation $\rho_{\rm ind}=\chi\cdot\phi_{\rm ext}$ is equivalent to $\rho_{\rm ind}(\mathbf{r})=\int\chi(\mathbf{r},\mathbf{r}',\omega)\phi_{\rm ext}(\mathbf{r}')d^3r'$. The field due to this induced charge is given by $\phi_{\rm ind}=V\chi\phi_{\rm ext}$, where $V(\mathbf{r},\mathbf{r}')=1/|\mathbf{r}-\mathbf{r}'|$ is the Coulomb potential. In terms of this density response function it follows that the surface dielectric function is given by[1]

$$g(\mathbf{q}_\parallel,\omega)=\frac{2\pi}{q_\parallel A}\int\int d^3r\,d^3r'\exp(i\mathbf{q}_\parallel\cdot\mathbf{r}_\parallel-i\mathbf{q}_\parallel\cdot\mathbf{r}'_\parallel+q_\parallel z+q_\parallel z')\chi(\mathbf{r},\mathbf{r}',\omega)\ , \tag{3}$$

where the integrals are over the half space $z<0$ and A is the surface area of the solid. We use Hartree atomic units throughout. The density response function can in turn be written in terms of the many-body ground state $|0\rangle$ and the excited states $|n\rangle$ of the solid:[13]

$$\mathrm{Im}[\chi(\mathbf{r},\mathbf{r}',\omega)]=\sum_n\langle 0|\hat\rho(\mathbf{r})|n\rangle\langle n|\hat\rho(\mathbf{r}')|0\rangle\pi\delta(\epsilon_n-\epsilon_0-\omega)\ , \tag{4}$$

with $\omega>0$ and where $\hat\rho(\mathbf{r})$ is the density operator of the solid (the real part of χ can be found by a Kramers-Kronig relation).

Obviously, if we are to calculate the surface dielectric function it is impractical to use Eq. (4) directly since it requires knowledge of the exact many-body eigenstates, and so we must make some approximation for the density response function χ. A suitable approximation is provided by the time-dependent Hartree[13] [or random-phase approximation (RPA)], to linear response theory, which relates χ to the single particle response function χ^0, defined by

$$\chi^0(\mathbf{r},\mathbf{r}',\omega)=\sum_{\alpha,\alpha'}\psi_\alpha(\mathbf{r})\psi^*_{\alpha'}(\mathbf{r})\psi_\alpha(\mathbf{r}')\psi^*_{\alpha'}(\mathbf{r}')\frac{n_\alpha-n_{\alpha'}}{\varepsilon_\alpha-\varepsilon_{\alpha'}-i\delta}\ , \tag{5}$$

where $\psi_\alpha(\mathbf{r})$ is a single particle eigenstate with energy ε_α and occupation number n_α. We can use the RPA to express the dielectric function $g(\mathbf{q},\omega)$ in terms of χ^0. We have, making use of the matrix notation used above,

$$\begin{aligned}g(\mathbf{q}_\parallel,\omega)&=(2\pi/q_\parallel A)\phi^\dagger_{\rm ext}\cdot\chi\cdot\phi_{\rm ext}\\&=(2\pi/q_\parallel A)\phi^\dagger_{\rm ext}\cdot\chi^0\cdot\phi\\&=(2\pi/q_\parallel A)\phi^\dagger\cdot(1-\chi^{0\dagger}V)\cdot\chi^0\cdot\phi\ .\end{aligned} \tag{6}$$

Here the potential ϕ is the total field, $\phi=\phi_{\rm ext}+\phi_{\rm ind}$, induced when the solid is subjected to an external potential $\phi_{\rm ext}=\exp(i\mathbf{q}_\parallel\cdot\mathbf{r}+q_\parallel z)$. The first line in Eq. (6) is just a rewriting of Eq. (3) and we are making use of the standard RPA results[13] that $\rho_{\rm ind}=\chi\cdot\phi_{\rm ext}=\chi^0\cdot\phi$ and that $\phi=(1-V\chi^0)^{-1}\phi_{\rm ext}$ in subsequent lines. Finally, taking the imaginary part of the last line in Eq. (6), the second term in the parentheses does not contribute and we obtain the following result, first derived by Persson and Zaremba:[1]

$$\mathrm{Im}[g(\mathbf{q}_\parallel,\omega)]=\frac{2\pi^2}{q_\parallel A}\sum_{\alpha,\alpha'}|\langle\psi_\alpha|\phi|\psi_{\alpha'}\rangle|^2\times(n_\alpha-n_{\alpha'})\delta(\varepsilon_\alpha-\varepsilon_{\alpha'}-\omega)\ , \tag{7}$$

giving $\mathrm{Im}[g(\mathbf{q},\omega)]$ in terms of the single-particle wave functions $|\psi_\alpha\rangle$ of the solid. It is this equation which connects the surface dielectric function to the band structure of the solid.

Equation (7) still does not provide a complete solution to the problem, since the potential ϕ is not known in general, and indeed can only be calculated *a priori* by inverting the full dielectric matrix to solve $\phi=\epsilon^{-1}\phi_{\text{ext}}=(1-V\chi^0)^{-1}\phi_{\text{ext}}$. However it is possible to approximate ϕ using, for example, its known small $\mathbf{q}$ limit, and thus to obtain an approximation for the surface response function $\text{Im}[g(\mathbf{q},\omega)]$ in the small $\mathbf{q}$ region. For small $\mathbf{q}$ we can take ϕ from the classical dielectric model, where the surface is treated as a uniform dielectric terminated at $z=0$. This model gives

$$\phi=[1-g(0,\omega)]\exp(i\mathbf{q}_\parallel\cdot\mathbf{r}_\parallel+q'_\parallel z) \tag{8}$$

for $z<0$, where $q'_\parallel=q_\parallel\sqrt{(\epsilon_1/\epsilon_3)}$ and the zero wave-vector response function $g(0,\omega)$ can be found from the bulk dielectric constants (determined experimentally or theoretically) using Eq. (2). This approximation for ϕ is equivalent to Persson and Zaremba's "bulk" approximation[1] since it gives ϕ correctly far inside the surface. Equation (8) does not give a good description of the potential ϕ very close to the surface. For small z there is in addition a "surface" potential which gives the difference between the true potential ϕ and Eq. (8). However the surface term gives a contribution to the integral in Eq. (7) which is of order $q_\parallel$ smaller than the bulk term, since for small $q_\parallel$ the matrix element integrals $\langle\psi_\alpha|\phi|\psi_{\alpha'}\rangle$ in Eq. (7) are dominated by the behavior of ϕ in the bulk. We shall thus neglect the surface terms, and simply use the bulk term, Eq. (8), in our calculations. For a metallic surface this would not be a good approximation, since at frequencies below the surface plasmon frequency ω_p the bulk contributions are also small because $g(0,\omega)$ is very close to unity, and so it is necessary to include both the surface and bulk contributions. However for graphite, as we shall see below, the bulk contributions are large and it is valid to neglect the surface term.

SURFACE DIELECTRIC RESPONSE OF GRAPHITE: THEORY

Since it is necessary to know the electron eigenstates ψ_α and band energies ε_α of graphite in order to evaluate the surface dielectric function, we shall give a brief summary of the electronic structure here. Graphite consists of layers of carbon atoms arranged in a hexagonal honeycomb structure; the hexagon side is $a/\sqrt{3}$ and the interlayer separation is $c/2$, where $a=2.46$ Å and $c=6.74$ Å. The carbon atoms form sp^2 hybrids giving strong bonds within each layer and giving rise to the graphite σ bands. The remaining p_z orbitals point normal to the layers and give rise to the π bands of graphite. It is the π bands which lie close to the Fermi level that give graphite its distinctive semimetallic behavior. For a single graphite layer the symmetry group leads to a degeneracy of the π bands at the corner of the hexagonal Brillouin zone[14–16] (the K point), and near the K point the bands have the following linear dispersion relation:

$$\varepsilon(\mathbf{k})=\pm p_0|\boldsymbol{\kappa}|\ , \tag{9}$$

where $\boldsymbol{\kappa}$ is the two-dimensional wave vector measured from the K point. The Fermi energy lies precisely at the K point, and thus the Fermi surface consists of a single point and there is zero density of states at the Fermi level. Having zero density of states at the Fermi energy but also no energy gap defines a semimetal. For three-dimensional graphite when the interaction between the graphite layers is taken into account, there is a slight dispersion with wave vector k_z parallel to the c axis. In a tight-binding approximation with nearest-neighbor interactions the π band energies become modified to[15]

$$\begin{aligned}\varepsilon_{1\pm}(\mathbf{k})&=+\gamma_1\Gamma/2\pm[(\gamma_1^2\Gamma^2/4+\gamma_0^2|S|^2)]^{1/2}\ ,\\ \varepsilon_{2\pm}(\mathbf{k})&=-\gamma_1\Gamma/2\pm[(\gamma_1^2\Gamma^2/4+\gamma_0^2|S|^2)]^{1/2}\ ,\end{aligned} \tag{10}$$

giving four distinct bands. Here $S=\exp(-ik_xa/\sqrt{3})+2\cos(k_ya/2)\exp(2ik_xa/\sqrt{3})$ and $\Gamma=2\cos(k_zc/2)$. In the vicinity of the K point $\gamma_0^2|S|^2\approx p_0^2\kappa^2$ where $\boldsymbol{\kappa}$ is the parallel wave vector measured relative to the K point and $p_0=\frac{1}{2}\sqrt{3}a\gamma_0$, and the bands are hyperbolic approaching the asymptotic slope p_0 but with energies 0 or $\pm\gamma_1\Gamma$ at the K point. γ_0 and γ_1 are tight-binding parameters which can be estimated from self-consistent band-structure calculations[17] giving the values $\gamma_0=2.0$ eV and $\gamma_1=0.4$ eV. The band structure in the vicinity of the K point is shown in Fig. 1 together with the three-dimensional (3D) Brillouin zone, which is a hexagonal prism. From the bands in Eq. (10) we see that the Fermi surface consists of lines along the vertical prism edges HKH of the zone. This line Fermi surface gives the typical semimetallic zero density of states at the Fermi energy with no energy gap. More accurate band calculations show that this line Fermi surface widens slightly to form a thin Fermi surface with a small but nonzero density of states;[18] however, this correction is not important here since it is only relevant at very small energies, $\ll 0.1$ eV.

To calculate the surface dielectric function using Eq. (7) we need to obtain the wave functions ψ_α of semi-infinite graphite. These can be obtained from the bulk Bloch functions, which are of the form

$$\Psi_{\gamma\mathbf{k}}(\mathbf{r})=(N)^{-1/2}\sum_i\lambda_\gamma(\mathbf{k})\psi_p(\mathbf{r}-\mathbf{r}_i)\exp(i\mathbf{k}\cdot\mathbf{r}_i)\ , \tag{11}$$

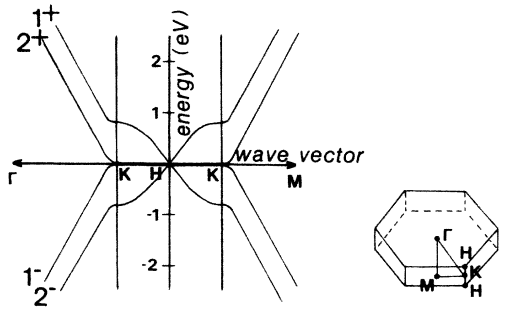

FIG. 1. Band structure of graphite near the K point, and the 3D Brillouin zone.

where $\psi_p(\mathbf{r}-\mathbf{r}_i)$ is the atomic p_z orbital at site i; there are N sites in the solid. γ is a band index. Now, since graphite consists of layers which only interact via nearest-neighbor interactions, the effect of the surface is to act as a simple reflecting barrier at $z=0$ for the bulk Bloch states. The wave functions of semi-infinite graphite are thus given by

$$\psi_{\gamma\mathbf{k}}(\mathbf{r})=(2/N)^{1/2}\sum\lambda_\gamma(\mathbf{k})\psi_p(\mathbf{r}-\mathbf{r}_i)\exp(i\mathbf{k}\cdot\mathbf{r}_i)\sin(k_z z_i)\ . \tag{12}$$

With these wave functions and the potential given in Eq. (8) it is possible to evaluate the response function $g(\mathbf{q}_\parallel,\omega)$ from Eq. (7). First, however, it is helpful to make one further simplification: we are interested in values of $q_\parallel$ small compared to the size of the Brillouin zone and so we can make a dipole approximation, i.e., treat the potential ϕ as varying slowly on the scale of the unit cell. The interband transitions will then be near to vertical and can be written in terms of optical oscillator strengths. This results in

$$\mathrm{Im}[g(q_\parallel,\omega)]=|1-g(0,\omega)|^2\frac{1}{2\pi q_\parallel q_\parallel'}\sum_{\gamma,\gamma'}\int d^3k\frac{1}{2\omega}[q_\parallel^2 f_\parallel^{\gamma\gamma'}(\mathbf{k})+q_\parallel'^2 f_\perp^{\gamma\gamma'}(\mathbf{k})]\delta(\epsilon_{\gamma'}(\mathbf{k}+\tfrac{1}{2}\mathbf{Q})-\epsilon_\gamma(\mathbf{k}-\tfrac{1}{2}\mathbf{Q})-\omega)\ , \tag{13}$$

with $\mathbf{Q}=(\mathbf{q}_\parallel,0)$. Since the bands are close to being cylindrically symmetric near the K point, the response function depends only on the modulus of $\mathbf{q}_\parallel$, not on its direction, and we shall subsequently treat $\mathrm{Im}[g(q_\parallel,\omega)]$ as a function of a scalar argument $q_\parallel$. $f_\parallel^{\gamma\gamma'}(\mathbf{k})$ and $f_\perp^{\gamma\gamma'}(\mathbf{k})$ are the dipole oscillator strengths parallel and perpendicular to the graphite layers, respectively, defined by

$$f^{\gamma\gamma'}(\mathbf{k})=2\frac{|\langle\psi_{\gamma k}|\mathbf{e}\cdot\mathbf{p}|\psi_{\gamma k}\rangle|^2}{\epsilon_{\gamma'}(\mathbf{k}')-\epsilon_\gamma(\mathbf{k})}\ , \tag{14}$$

where e is the polarization vector. These dipole oscillator strengths can be calculated within the tight-binding approximation, giving for polarizations parallel to the layers[19,20]

$$f_\parallel^{\gamma\gamma'}(\mathbf{k})=\frac{p_0^2\gamma_0^2|S|^2}{S_{\gamma'}S_\gamma}\frac{(E_{\gamma'}\pm E_\gamma)^2}{(E_{\gamma'}-E_\gamma)}\ , \tag{15}$$

the plus sign holding for transitions between the bands $1-$ to $1+$ and $2-$ to $2+$, and the minus sign holding for transitions $1-$ to $2+$ and $2-$ to $1+$ [using the band labeling of Eq. (10) and Fig. 1]. Here $S_\gamma=E_\gamma^2+\gamma_0^2|S|^2$. For transitions polarized perpendicular to the layers we find

$$f_\perp^{\gamma\gamma'}(\mathbf{k})=\frac{8p_1^2}{S_{\gamma'}S_\gamma}\frac{E_{\gamma'}^2E_\gamma^2}{(E_{\gamma'}-E_\gamma)}\sin^2(k_z c/2) \tag{16}$$

for interband transitions $1-$ to $1+$ and $2-$ to $2+$, and zero otherwise. The quantity p_1 is a matrix element of the dipole operator between carbon p_z orbitals on adjacent layers. Calculating this interatomic matrix element numerically using Hartree-Fock atomic wave functions for carbon, we estimate p_1 as 0.049 in atomic units. The band slope parameter p_0 can also be calculated from interatomic dipole matrix elements, since the band structure near the K point can be derived from $\mathbf{k}\cdot\mathbf{p}$ perturbation theory. This calculation gives $p_0=0.325$, in atomic units, which is consistent with the estimate of 0.29 found from the self-consistent band structure. In practice the parallel oscillator strengths $f_\parallel^{\gamma\gamma'}(\mathbf{k})$ were much larger than the perpendicular ones and dominated the surface response function.

We have evaluated the surface dielectric function $\mathrm{Im}[g(q_\parallel,\omega)]$ for graphite using Eq. (13). This was accomplished by performing a numerical integration over the surface in $\mathbf{k}$ space defined by $\epsilon_{\gamma'}(\mathbf{k}+\frac{1}{2}\mathbf{Q})-\epsilon_\gamma(\mathbf{k}-\frac{1}{2}\mathbf{Q})=\omega$. The calculation could be simplified somewhat by exploiting the near cylindrical symmetry and hyperbolic behavior of the bands near the K point, which makes the surface $\epsilon_{\gamma'}(\mathbf{k}+\frac{1}{2}\mathbf{Q})-\epsilon_\gamma(\mathbf{k}+\frac{1}{2}\mathbf{Q})=\omega$ an ellipsoid in $\mathbf{k},\Gamma$ coordinates [Γ defined after Eq. (10)]. The quantity $|1-g(0,\omega)|^2$ was estimated using the classical electrostatic result of Eq. (2) and values of the bulk dielectric constants $\epsilon_1(\omega)$ and $\epsilon_3(\omega)$ available in the literature.[21–23] It was found that $|1-g(0,\omega)|$ was fitted to a good approximation by the function $0.3\tanh(\omega/0.975\ \text{eV})$, and that $q_\parallel'/q_\parallel=\sqrt{(\epsilon_1/\epsilon_3)}\sim 2.1-0.27\omega$ at the energies of interest. The results of this calculation of the surface dielectric function $\mathrm{Im}[g(q_\parallel,\omega)]$ are described below.

SURFACE DIELECTRIC RESPONSE OF GRAPHITE: RESULTS

The calculated surface dielectric function $\mathrm{Im}[g(q_\parallel,\omega)]$ at $q_\parallel=0$ is shown in Fig. 2. We have compared the calculated function with the values of $\mathrm{Im}[g(0,\omega)]$ obtained using the experimental bulk dielectric constants $\epsilon_1(\omega)$ and $\epsilon_3(\omega)$ and the classical electrostatic result of Eq. (2). We can see from the figure that the calculated dielectric function remains roughly constant over the energy range 1.5–3 eV, in good qualitative agreement with the experimental values. The overall magnitude of the calculated response function in this range is typically 0.15, while the experimental values are around 0.19. The origin of this difference is that in the self-consistent band structure of graphite[17,24] the $1+$ band (Fig. 1) has a much smaller slope than given by the tight-binding bands in Eq. (10) (and in fact the $1+$ band crosses the $2+$ band becoming lower in energy at the M point). Such a lower slope would imply a larger joint density of states for transitions into the $1+$ band, thus enhancing the overall value of $\mathrm{Im}[g(q_\parallel,\omega)]$. The slight discrepancy between the tight-binding calculation and experiment in the overall magnitude of $\mathrm{Im}[g(q_\parallel,\omega)]$ would not affect

the EELS spectra significantly since only relative intensities can be measured accurately. In Fig. 2 we can also see that the response function shows a sharp feature at 0.8 eV. This corresponds to transitions between the flat regions of the bands at the K point which are split by $2\gamma_1=0.8$ eV. There appears to be no experimental determinations of the bulk dielectric functions $\epsilon_1(\omega)$ and $\epsilon_3(\omega)$ at this energy which could confirm the existence of this feature, but infrared optical reflectance spectra do show some structure at around 0.8 eV (Refs. 25 and 26) which is attributed to these interband transitions at the K point.

For comparison we have also plotted the $q_\parallel=0$ surface response function of aluminum in Fig. 2. This was obtained from the bulk dielectric function $\epsilon(\omega)$ determined optically.[27] The points plotted for aluminum have been multiplied by a factor of 5, to make the values visible on the same graph as for graphite. It is thus clear from the figure that for aluminum the surface response function is substantially weaker than it is for graphite; this is also true for other metals. It is because the response function $\mathrm{Im}[g(q_\parallel,\omega)]$ is so much larger for graphite than for metals that the EELS spectrum is so much more intense. The interpretation is clear, namely, for graphite it is possible to have vertical transitions between the π bands at these infrared energies, while for most metals there are no vertical transitions at such low energies. In other words, for a graphite surface a large part of the oscillator strength in $\mathrm{Im}[g(q_\parallel,\omega)]$ occurs at much lower energies than for metals, because of the semimetallic band structure. This is the opposite of what one might at first expect, namely, that the low density of states for the semimetal would imply only a small oscillator strength at low energies, and that the response would thus be weak as for a semiconductor.

The wave-vector dependence of the calculated dielectric function $\mathrm{Im}[g(q_\parallel,\omega)]$ is shown in Fig. 3. The most important feature here is the existence of a sharp cutoff effect where the imaginary part of the dielectric function becomes zero at small frequencies when $q_\parallel\neq 0$. The origin of this effect can be seen most simply in terms of the two-dimensional single layer graphite band structure of Eq. (9) in which the band energies are $\varepsilon(\kappa)=\pm p_0\kappa$ near the K point. It is easy to see from this band structure that transitions of frequency ω and wave vector $q_\parallel$ can only occur if $\omega/q_\parallel\geq p_0$. If $\omega/q_\parallel<p_0$ there are no possible transitions which connect occupied and unoccupied bands. This is apparent if we consider the surface in 2D k space of the allowed transitions; this satisfies $\omega=|\boldsymbol{\kappa}+\frac{1}{2}\mathbf{q}_\parallel|+|\boldsymbol{\kappa}-\frac{1}{2}\mathbf{q}_\parallel|$ and is thus an ellipse with foci at $\pm\frac{1}{2}\mathbf{q}_\parallel$ and eccentricity $p_0q_\parallel/\omega$. We thus require $p_0q_\parallel/\omega<1$. This condition implies that the dielectric function would be zero if $\omega<p_0q_\parallel$, roughly as seen in Fig. 3. In fact when we include the more complicated band structure of Eq. (2), which allows for interlayer interactions, the cutoff condition becomes modified to $\omega<p_0q_\parallel-2\gamma_1$, which is what is seen in Fig. 3 ($2\gamma_1=0.8$ eV). The sharp peaked structure that develops in $\mathrm{Im}[g(q_\parallel,\omega)]$ near the cutoff that can be seen in Fig. 3 can also be explained in terms of the simple 2D band structure $\varepsilon(\kappa)=\pm p_0\kappa$, since in this model the joint density of states for transitions with frequency ω and wave vector $q_\parallel$ has an inverse square root singularity at the cutoff when $p_0q_\parallel/\omega=1$.

RESULTS: EELS SPECTRA OF GRAPHITE

Using the surface response function from Eq. (13) we have calculated the EELS spectra of graphite. The comparison between theory and experiment is shown in Fig. 4. The theoretical intensities were obtained using the standard dipole scattering formula:[2,6,7]

$$P(\mathbf{k},\mathbf{k}')=\frac{2}{\pi^2}\frac{k'}{k\cos(\theta_i)}\frac{q_\parallel}{(q_\parallel^2+q_\perp^2)^2}\mathrm{Im}[g(q_\parallel,\omega)]\ , \qquad (17)$$

where $P(\mathbf{k},\mathbf{k}')d\Omega_{\mathbf{k}'}d\omega$ is the probability of scattering from state $\mathbf{k}$ to within a solid angle element $d\Omega_{\mathbf{k}'}$ around the direction of $\mathbf{k}'$ and with energy losses between ω and $\omega+d\omega$. Here θ_i is the angle of incidence, $\mathbf{q}_\parallel=\mathbf{k}_\parallel-\mathbf{k}'_\parallel$, and $q_\perp=k_z-k'_z$. The final EELS spectrum was obtained by integrating $P(\mathbf{k},\mathbf{k}')$ over the detector aperture (assumed to be 1.25° half-angle). A simple derivation of

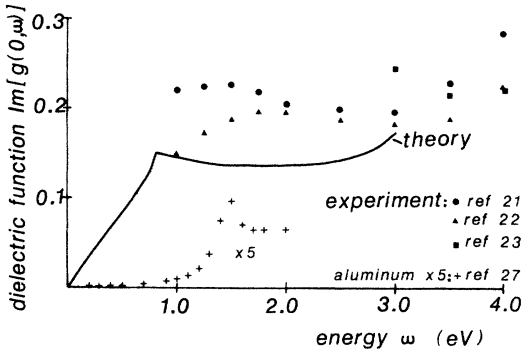

FIG. 2. Calculated surface dielectric function for graphite at zero parallel wave vector, $\mathrm{Im}[g(0,\omega)]$, and comparison with values obtained from experimental bulk dielectric functions $\epsilon_1(\omega)$ and $\epsilon_3(\omega)$ (Refs. 21–23). The surface response function for aluminum (Ref. 27) is also shown, where each point has been multiplied by a factor of 5.

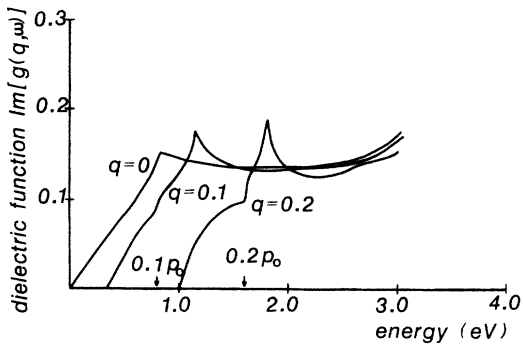

FIG. 3. Parallel wave-vector dependence of the surface dielectric function of graphite $\mathrm{Im}[g(\mathbf{q}_\parallel,\omega)]$. Note the existence of a cutoff region below $\omega=p_0q_\parallel$, which is due to the finite slope of the bands, p_0, at the K point.

Eq. (17) is given in the Appendix in order to demonstrate why it is that the EELS intensity is directly related to the imaginary part of the surface dielectric function.

The experimental EELS intensities and the results of the calculation have been described elsewhere;[9] however, for completeness we summarize the main points here. Figure 4(a) shows the theoretical and experimental loss intensities on the specular direction, calculated assuming a 9 eV electron beam incident at 65° to the normal. The broad continuum of electron-hole pair excitations seen in the experiment is well reproduced by the theory. As mentioned above, the unusually high intensity of the spectrum is explained in the calculation by the large size of $\mathrm{Im}[g(q_{\parallel},\omega)]$ for graphite compared typical metals. Because of the unknown detector efficiency and crystal reflectivity, the absolute experimental magnitude could not be obtained accurately and so each theory curve has been normalized to give the best rms fit to the data.

The spectrum taken at 5° and 10° towards the surface normal are shown in Figs. 4(b) and 4(c). Here the continuum of losses rises in intensity at small energies before falling again giving a single broad maximum. This maximum in intensity is reproduced by the theory. The reason the intensity is small at low energies is the band structure cutoff effect described above in which the response function $\mathrm{Im}[g(q_{\parallel},\omega)]$ is zero if $\omega < p_0 q_{\parallel}$. For nonspecular scattering the parallel wave vector $q_{\parallel}$ is finite at $\omega=0$, and so at low energies the cutoff condition is satisfied and there should be no inelastic scattering. [Note that the spectra shown in Figs. 4(b) and 4(c) have had a background subtracted arising from diffuse elastic scattering combined with energy loss, as discussed in Ref. 9.]

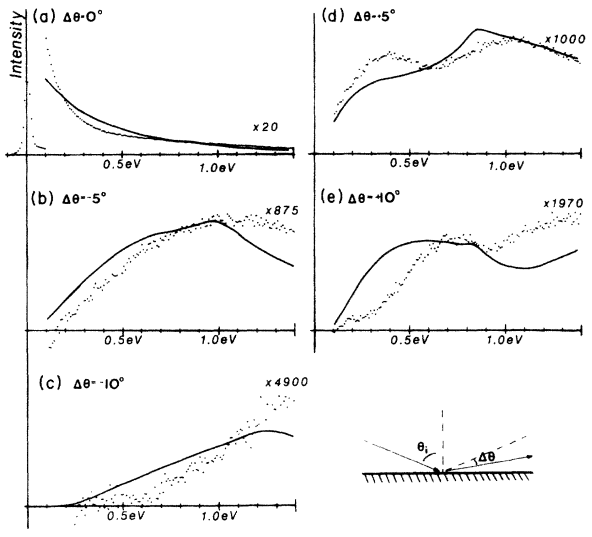

FIG. 4. Theoretical and experimental EELS intensities for the graphite surface. (a) shows the specular spectrum, (b) and (c) the spectra at 5° and 10° towards the surface normal, respectively, and (d) and (e) show the spectra at 5° and 10° away from the surface normal. A background due to diffuse elastic scattering has been subtracted from the data, as described in Ref. 9. Each theoretical curve is normalized to give the best rms agreement with the experiment.

The spectra taken at 5° and 10° to the surface normal are shown in Figs. 4(d) and 4(e). The shape is now more complicated and instead of a single maximum in intensity there is now a two-peaked structure. As explained in Ref. 9, this double maximum is a combination of two factors: firstly, the band structure cutoff effect gives a single broad maximum in intensity, just as in Figs. 4(b) and 4(c). However, in addition there is a further minimum in intensity because the dipole scattering intensity of Eq. (17) becomes zero whenever $q_{\parallel}=0$ provided $q_{\perp}\neq 0$. This kinematical condition only occurs for nonspecular scattering, when the scattering angle is towards the surface normal, hence explaining why the nonspecular spectra in Figs. 4(d) and 4(e) show this additional minimum while the spectra in Figs. 4(b) and 4(c) do not. The dispersion of this minimum with angle from specular can be calculated easily and agrees well with the experimental dispersion.[9] The theoretical spectra in Figs. 4(d) and 4(e) reproduce all the features of the experimental results, at least qualitatively. The lack of a more precise agreement could be due to a number of factors, including experimental uncertainties in the scattering angles, a slight tilt of the crystal which would lead to out of plane scattering, and uncertainty in the beam energy due to small work-function differences between the sample and the beam source. The existence of this extra minimum in intensity for nonspecular scattering is not peculiar to graphite but should be observable in principle on any substrate. However the effect is only strong enough to be observed on graphite because of the high intensity of the spectrum.

To conclude, we have shown it is possible to calculate a surface dielectric function for a material which is not a simple free-electron metal. This shows how the unusual surface dielectric properties of graphite can be understood in terms of the semimetallic band structure. Theoretical EELS spectra, based on dipolar scattering and the calculated surface dielectric function for graphite, reproduce all the principal features of the spectra including the high intensity on specular compared to a metal and also the unusual dispersing features seen in the nonspecular spectra.

ACKNOWLEDGMENTS

This work is funded by the Science and Engineering Research Council of the U.K. JFA and REP would like to thank, respectively, Emmanuel College, Cambridge and the Royal Commission for the Exhibition of 1851 for financial support.

APPENDIX

It is useful to see how the relationship between the EELS intensities and the surface dielectric function given in Eq. (17) comes about, since this shows why the surface dielectric function is the important quantity describing the surface in EELS. Consider the EELS electron moving freely in the half-space $z>0$ and

reflected by an infinite barrier at $z=0$; its wave function is then $|\mathbf{k}\rangle = 2^{1/2}\sin(k_z z)\exp(i\mathbf{k}\cdot\mathbf{r})$ with $k_z > 0$. The inelastic scattering arises because the Coulomb potential of the electron provides a perturbation of the solid which can excite it out of the ground state. If the solid is initially in its ground state $|0\rangle$, then the rate at which the Coulomb interaction, V, excites the substrate to state $|n\rangle$ scattering the electron to state $|\mathbf{k}'\rangle$ is given by Fermi's golden rule:

$$\Gamma_{\mathbf{k}\mathbf{k}'} = 2\pi \sum_n |\langle 0,\mathbf{k}|\hat{V}|n,\mathbf{k}'\rangle|^2 \delta(\varepsilon_{\mathbf{k}'}+\varepsilon_n-\varepsilon_{\mathbf{k}}-\varepsilon_0) , \quad \text{(A1)}$$

where $|n\rangle$ is an excited eigenstate of the solid with energy ε_n, $\varepsilon_k = \frac{1}{2}k^2$, etc. The inelastic scattering probability of an electron reflected from the surface is found by dividing $\Gamma_{\mathbf{k}\mathbf{k}'}$ by the incident flux $k_z/\sqrt{2}$. Now, since V is a Coulomb operator,

$$\hat{V} = \int d^3r\, d^3r' \frac{\hat{\rho}_e(\mathbf{r})\hat{\rho}_s(\mathbf{r}')}{|\mathbf{r}-\mathbf{r}'|} , \quad \text{(A2)}$$

where $\hat{\rho}_e(\mathbf{r})$ and $\hat{\rho}_s(\mathbf{r}')$ are the density operators for the incoming probe electron and for the solid, respectively, the Fermi golden rule expression of Eq. (A1) contains factors of the form

$$\sum_n \langle 0|\hat{\rho}(\mathbf{r})|n\rangle\langle n|\hat{\rho}(\mathbf{r}')|0\rangle \pi\delta(\epsilon_n-\epsilon_0-\omega) , \quad \text{(A3)}$$

which is just the density response function $\mathrm{Im}[\chi(\mathbf{r},\mathbf{r}',\omega)]$ defined in Eq. (4). It is because the EELS intensity is proportional to this density response function that we find the relation between EELS intensities and the dielectric properties of the solid. In fact, if we define the surface response function by Eq. (3), and make use of the 2D Fourier transform of the Coulomb potential, $2\pi/q_\parallel \exp(i\mathbf{q}_\parallel\cdot\mathbf{r}_\parallel - q_\parallel|z-z'|)$, we find that the scattering rate above leads to

$$P(\mathbf{k},\mathbf{k}') = \frac{2}{\pi^2}\frac{k'}{k\cos(\theta_i)}\frac{1}{q_\parallel}\left[\frac{q_\parallel}{q_\parallel^2+q_\perp^2} - \frac{q_\parallel}{q_\parallel^2+q_\perp'^2}\right] \times \mathrm{Im}[g(q_\parallel,\omega)] \quad \text{(A4)}$$

(with $q_\perp = k_z - k_z'$ and $q_\perp' = k_z + k_z'$), and we recover the usual result given in Eq. (17) (the second term in the square brackets can be dropped since it is small). The dipole scattering expression, (A4), is entirely analogous to the usual result in bulk EELS (Ref. 21) relating the spectrum to the bulk loss function $\mathrm{Im}[-1/\epsilon(\omega)]$.

[1] B. N. J. Persson and E. Zaremba, Phys. Rev. B **31**, 1863 (1985).
[2] B. N. J. Persson, Phys. Rev. Lett. **50**, 1089 (1983).
[3] P. M. Echenique, R. H. Ritchie, N. Barberan, and J. Inkson, Phys. Rev. B **23**, 6486 (1981).
[4] J. F. Annett and P. M. Echenique, Phys. Rev. B **34**, 6853 (1986).
[5] J. F. Annett and P. M. Echenique, Phys. Rev. B **36**, 8986 (1987).
[6] S. Andersson, B. N. J. Persson, M. Persson, and N. D. Lang, Phys. Rev. Lett. **52**, 2073 (1984).
[7] S. Andersson and B. N. J. Persson, Phys. Rev. Lett. **50**, 2028 (1983).
[8] B. N. J. Persson and J. E. Demuth, Phys. Rev. B **30**, 5968 (1984).
[9] R. E. Palmer, J. F. Annett, and R. F. Willis, Phys. Rev. Lett. **58**, 2490 (1987).
[10] R. E. Palmer, J. F. Annett, and R. F. Willis, 9th European Conference on Surface Science, Lucerne, 1987 [Surf. Sci. **189/190**, 1009 (1987)].
[11] G. Binnig, H. Fuchs, Ch. Gerber, H. Rohrer, E. Stoll, and E. Tosatti, Europhys. Lett. **1**, 31 (1986); J. Tersoff, Phys. Rev. Lett. **57**, 440 (1986); J. M. Soler, A. M. Baro, N. Garcia, and H. Rohrer, *ibid.* **57**, 444 (1986).
[12] D. Tomanek, S. G. Louie, H. J. Manin, D. W. Abraham, R. E. Thompson, E. Gaz, and J. Clarke, Phys. Rev. B **35**, 7790 (1987).
[13] L. Hedin and S. Lundqvist, *Solid State Physics,* edited by H. Ehrenreich, F. Seitz, and D. Turnbull (Academic, New York, 1969), Vol. 23, p. 1.
[14] P. R. Wallace, Phys. Rev. **71**, 622 (1947).
[15] J. C. Slonczewski and P. R. Weiss, Phys. Rev. **109**, 272 (1958).
[16] G. S. Painter and D. E. Ellis, Phys. Rev. B **1**, 4747 (1970).
[17] N. A. W. Holzwarth, S. G. Louie, and S. Rabii, Phys. Rev. B **26**, 5382 (1982).
[18] J. W. McClure, Phys. Rev. **108**, 612 (1957).
[19] Y. H. Ichikawa and K. Kobayashi, Carbon **3**, 401 (1966).
[20] K. J. Kobayashi and Y. Uemura, J. Phys. Soc. Jpn. **25**, 404 (1968).
[21] J. Daniels, C. v. Festenberg, H. Raether, K. Zeppenfeld, *Springer Tracts in Modern Physics* (Springer-Verlag, Heidelberg, 1970), Vol. 54, p. 77.
[22] H. Venghaus, Phys. Status Solidi B **71**, 609 (1975).
[23] R. Klucker, M. Skibowski, and W. Steinmann, Phys. Status Solidi B **65**, 703 (1974).
[24] R. C. Tatar and S. Rabii, Phys. Rev. B **25**, 4126 (1982).
[25] E. A. Taft and H. R. Philipp, Phys. Rev. **138**, A197 (1965).
[26] W. Y. Liang (private communication).
[27] H. J. Hagamann, W. Gudat, and C. Kunz, DESY Report No. SR-74/7, 1974 (unpublished).